Available online at www.sciencedirect.com

SciVerse ScienceDirect

Ceramics International 39 (2013) S341–S344

CERAMICS INTERNATIONAL

www.elsevier.com/locate/ceramint

Parametric effects on femtosecond laser ablation of Al_2O_3 ceramics

Bor-Chyuan Chen[a,1], Yu-Hsiang Tsai[b], Ching-Yen Ho[b,*,1], Cheng-Sao Chen[b], Chuang Ma[b]

[a]Department of Chinese Medicine, Buddhist Dalin Tzu Chi General Hospital, Chiayi 622, Taiwan
[b]Department of Mechanical Engineering, Hwa Hsia Institute of Technology, Taipei 235, Taiwan

Available online 16 October 2012

Abstract

This paper investigates the effects of parameters on femtosecond laser ablation of Al_2O_3 ceramics. Ceramic alumina (Al_2O_3) is an important substrate used in hybrid circuits. Generally it is a difficult-to-cut material by conventional drilling and cutting procedures. Laser is suitable for precise form processing on hard or brittle ceramic materials, and with the increasing availability of femtosecond pulse lasers, the interest in using femtosecond laser ablation to produce precise, well-defined micrometer-sized structures in the ceramic materials is increasing. The laser parameters and material properties play an important role in the quality and efficiency of ceramics processing. This work develops a model to investigate parametric effects on femtosecond laser ablation of Al_2O_3 ceramics. The ablation depth and squared crater diameter per pulse predicted by this study are in agreement with the available experimental data. The effects of laser parameters and material properties on femtosecond laser ablation of Al_2O_3 ceramics are also discussed.

Keywords: A. Shaping; D. Al_2O_3; E. Thermal applications

1. Introduction

Laser micromachining is preferred because of fast material-processing speed, large scan area and single-step capability. With the increasing availability of femtosecond pulse lasers, femtosecond laser has many applications such as fabrication of MEMS/NEMS, CMOS, 3D-microstructures, micro-trenches, microchannels, microholes, periodical sub-micron gratings and nanophotonics [1–3].

It is commonly believed that one of the most important advantages of femtosecond laser ablation is that the energy deposited by ultrashort laser pulses does not have enough time to move into the interior of bulk sample. High-power femtosecond laser irradiation of materials involves many physical processes including electron and lattice energy absorbing and transportation, electron-phonon energy coupling and accumulation [4].

Ceramic alumina (Al_2O_3) is an important substrate used in hybrid circuits due to its high dielectric strength coupled with an excellent thermal stability and high thermal conductivity of 25 W $m^{-1}K^{-1}$. As conventional mechanical punching and stamping in these substrates becomes limited below dimensions of a few hundred micrometers, laser processing offers potential advantages including the elimination of tool wear.

If a laser is applied for ceramic material processing, it has the following advantages: non-conductive, hard or brittle material can be processed, small areas can be processed by a focused single pulse and no tool wear occurs [5,6]. Therefore, laser is suitable for precise form processing on difficult-to-cut materials. With the increasing availability of femtosecond pulse lasers, the interest in using femtosecond laser ablation to produce precise, well-defined micrometer-sized structures in the ceramic materials that cannot be satisfactorily treated with standard nanosecond lasers is increasing.

Parametric effects on femtosecond laser ablation of Al_2O_3 ceramics are analytically investigated in this paper. The understanding of parametric effects benefits the improvements of machining quality and efficiency as well as parameter selections.

2. Analysis

Considering a femtosecond laser-pulse irradiating semi-finite aluminum oxide ceramics (Al_2O_3), if the laser power is high enough, the aluminum oxide ceramics will be

*Corresponding author. Tel.: +886 2 89415059; fax: +886 2 29436521.
E-mail address: hcy2182@yahoo.com.tw (C.-Y. Ho).
[1]These authors contributed equally. (first author)

0272-8842/$ - see front matter
http://dx.doi.org/10.1016/j.ceramint.2012.10.090

ablated. Therefore the material removal occurs during the process.

Laser-induced ablation of a substrate and the laser beam propagating in the z-direction are taken into account. The pulse-laser intensity is supposed to a Gaussian profile and the phase transition is assumed to be from solid to vapor without melting. Based on the heat conduction equation with a reference frame attached to the surface $z=0$, a three-dimensional model can be written as

$$\frac{\partial T}{\partial t}=\alpha\left(\frac{\partial^2 T}{\partial x^2}+\frac{\partial^2 T}{\partial y^2}+\frac{\partial^2 T}{\partial z^2}\right)+\frac{q_L}{\rho c} \tag{1}$$

where T is the temperature in the workpiece. α represents thermal diffusivity. ρ and c denote mass density and heat capacity, respectively. x, y and z signify spatial coordinates. The symbol t stands for time. A 110 fs pulse laser with a wavelength of 790 nm is used to conduct this laser ablation of ceramics, in which the mode is TEM_{00} with the profile of the Gaussian distribution. The volumetric heating source q_L can be mathematically expressed as

$$q_L=\frac{(1-R)}{\delta}\frac{3Q}{\pi\sigma^2}\exp\left[-3\left(\frac{x^2+y^2}{\sigma^2}\right)-\frac{t^2}{\tau_0^2}-\frac{z}{\delta}\right] \tag{2}$$

where Q, R, δ and σ correspondingly represent the laser power, reflectivity, plasma absorption length and energy-distribution radius. 3 in Eq. (2) is taken to assure 90% of laser energy included within the energy-distribution radius. τ_0 symbolizes the laser pulse duration at FWHM. The temperature away from the laser irradiating location is supposed to be T_a (the ambient temperature). Hence the boundary conditions are

$$T(\pm\infty y, z, t)=T_a \quad \text{and} \quad T(x\pm\infty, z, t)=T_a \tag{3}$$

The boundary condition on the workpiece surface is set as

$$k\frac{\partial T(x,y,0,t)}{\partial z}=A_l\sigma_B\left(T^4-T_a^4\right)+h_c(T-T_a) \tag{4}$$

and

$$T(x,y,+\infty,t)=T_a \tag{5}$$

where k is the heat conductivity, A_l is the gray-scale coefficient, σ_B is the Stefan–Boltzman constant and h_c is the convection coefficient.

The initial condition is given as

$$T(x,y,z,0)=T_a \tag{6}$$

if the solid–vapor interface is expressed in the form

$$z=f(x,y,t) \tag{7}$$

the interface energy balance equation can be written as

$$q_L\delta+\left[1+\left(\frac{\partial f}{\partial x}\right)^2+\left(\frac{\partial f}{\partial y}\right)^2\right]\left[k\frac{\partial T}{\partial z}\right]=\rho\gamma\frac{\partial f}{\partial t}\,\mathrm{at}\,T=T_e \tag{8}$$

where γ is the latent heat of evaporation and T_e is the evaporation temperature.

3. Results and discussion

In order to validate this study, the analytical solutions of this analysis were compared with the available data from the experiments for ablation of aluminum oxide ceramics using femtosecond laser. The dimensional parameters used in this study include laser fluence F, energy-distribution radius σ, pulse duration τ_0 at FWHM, optical penetration depth δ, reflectivity R, evaporation latent heat γ, thermal diffusivity α, mass density ρ, heat capacity c, and evaporation temperature T_e. The typical values of F, σ, τ_0, δ, R, γ, α, ρ, c and T_e were correspondingly chosen to be 1,000,000 J/m^2, 10 µm, 110 fs, 66.6 nm, 0.75, 4,760,000 J/kg, 0.0001 m^2/s, 3970 kg/m^3, 10,000 J/kgK and 3700 K.

The effect of reflectivity on the ablated depth per pulse and squared crater diameter is shown in Fig. 1. The measured data [7] of ablation rate and squared crater diameter versus laser fluences are also plotted in Fig. 1. Fig. 1 indicates that the ablation rate and squared crater diameter predicted by this work are consistent with the available experimental data. The ablated depth and crater diameter per pulse increase with the decreasing reflectivity and increasing laser fluence. The squared crater diameter linearly increases with the logarithm of laser fluences.

Fig. 2 illustrates the relations of ablation rate and squared crater diameter with laser fluence for different optical penetration depths. The increase of the optical penetration depth leads to the decrease of squared crater

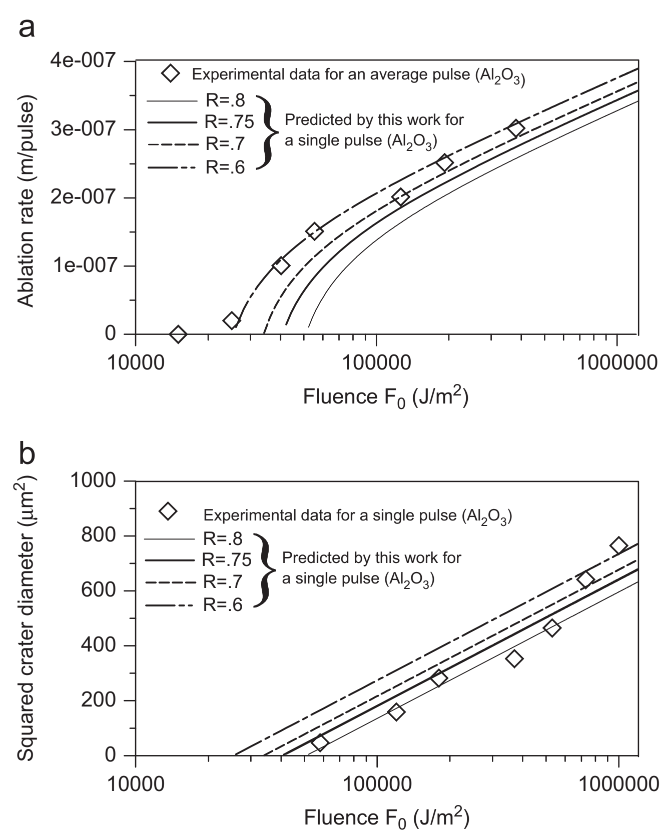

Fig. 1. Ablated depth per pulse and squared crater diameter versus laser fluence for different reflectivities.

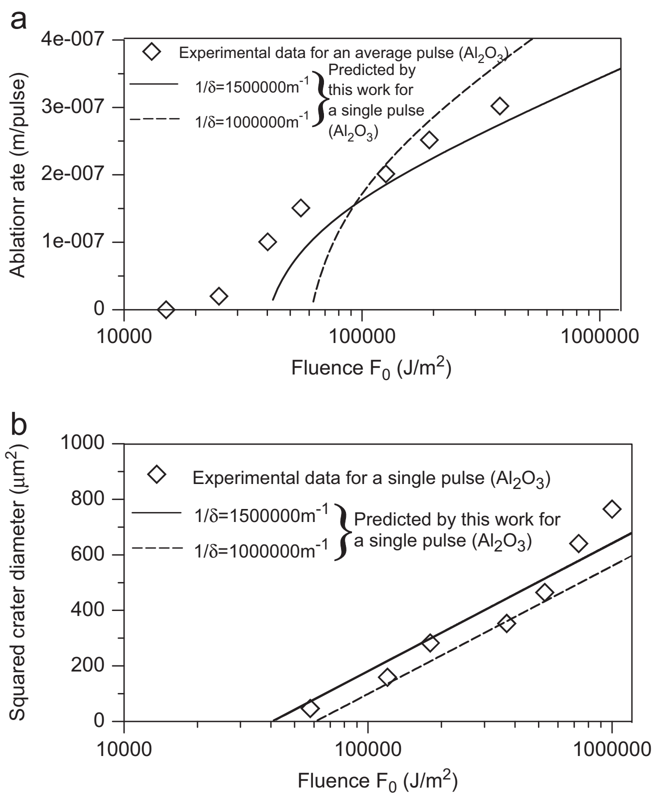

Fig. 2. Ablated depth per pulse and squared crater diameter versus laser fluence for different optical penetration depths.

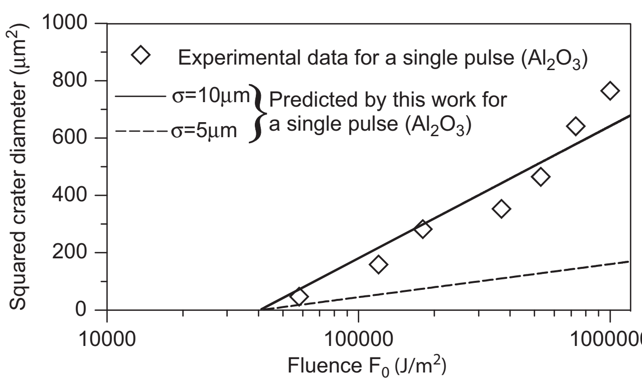

Fig. 3. Squared crater diameter versus laser fluence for different energy-distribution radii.

diameter. The possible reason is that the increase of energy penetrating along the direction of depth makes the energy on the surface decrease as the optical penetration depth increases.

However, for bigger optical penetration depth the material removal starts at higher fluence and the ablated depth per pulse is less at low laser fluences. The increase of the optical penetration depth enhances the energy penetrating into material but reduces the energy deposited on the surface. Therefore the material evaporation on the surface occurs more slowly for lower laser fluences.

The squared crater diameter versus laser fluence for different energy-distribution radii was sketched in Fig. 3.

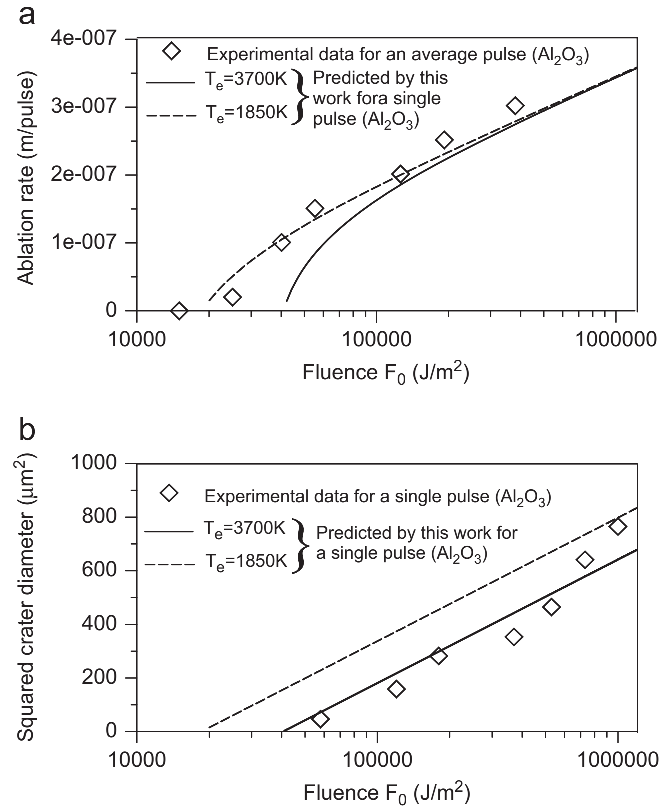

Fig. 4. Ablated depth per pulse and squared crater diameter versus laser fluence for different evaporation temperatures.

Energy-distribution radii obviously change the squared crater diameter. The small energy-distribution radius reduces the squared crater diameter. This is attributed to the nearly negligible heat diffusion along the radial direction in an ultrashort time.

Fig. 4(a) and (b), respectively, indicates the variations of ablation rate and squared crater diameter with fluence for different evaporation temperatures. The evaporation temperature influences the ablated depth per pulse at low laser fluences and squared crater diameter. The low evaporation temperature leads to the increase of the ablation rate at low laser fluences and increase of squared crater diameter.

Fig. 5 demonstrates how the relations of ablation rate and squared crater diameter to laser fluence vary with mass density. Unlike the evaporation temperature, small mass density increases the ablated depth and squared crater diameter per pulse for all laser fluences.

4. Conclusion

This paper studies the effect of material properties and laser parameters on the ablation rate and squared crater diameter for the femtosecond laser ablation of aluminum oxide ceramics. The ablation rate and squared crater diameter predicted by this work are consistent with those from the available experimental data. The ablation depth per pulse and the squared crater diameter increase with the

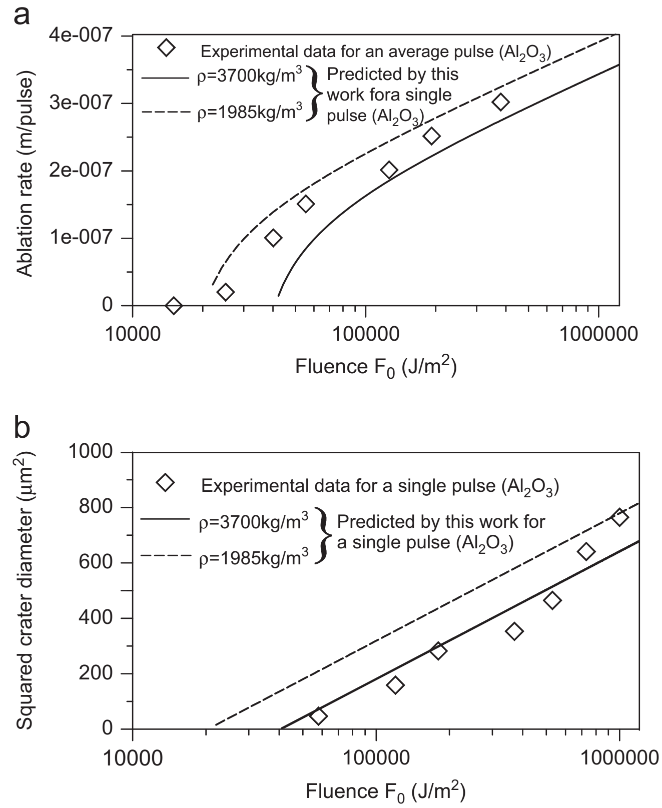

Fig. 5. Ablated depth per pulse and squared crater diameter versus laser fluence for different mass densities.

increasing laser fluences. The decrease of reflectivity enhances the ablated depth and squared crater diameter per pulse. For a large optical penetration depth, the increase of the energy penetrating into material reduces the energy deposited on the surface. Therefore the material removal occurs more slowly and the squared crater diameter decreases although the ablated depth per pulse increases. The energy-distribution radius obviously influences the squared crater diameter. The squared crater diameter also increases with the decreasing evaporation temperature. On the other hand, the decrease of evaporation temperature enhances the ablation depth per pulse only at low laser fluences. The small mass density increases the ablated depth and squared crater diameter per pulse for all laser fluences.

Acknowledgments

Support for this work by the National Science Council of the Republic of China under Grant no. NSC 99–2221-E-146-003 is gratefully acknowledged.

References

[1] R. Böhme, K. Zimmer, B. Rauschenbach, Direct laser etching of transparent materials: high-quality surface patterning and figuring formicro-optical applications, Proceedings of SPIE—The International Society for Optical Engineering 254 (2005) 1–9.

[2] S. Chen, V.V. Kancharla, Y. Lu, Laser-based microscale patterning of biodegrad-able polymers, International Journal of Materials and Product Technology 18 (2003) 457–468.

[3] J.L. Yang, J.L. Yu, Y.Y. Cui, Y. Huang, New laser machining technology of Al_2O_3 ceramic with complex shape, Ceramics International 38 (2012) 3643–3648.

[4] C.L. Guo, Thermal effects in femtosecond laser ablation of metals, Proceedings of SPIE—The International Society for Optical Engineering 6118 (2006) 61180801–61180814.

[5] M. Guillermin, F. Garrelie, N. Sanner, Single and multipulse formation of surface structures under static femtosecond irradiation, Applied Surface Science 253 (2007) 8075–8079.

[6] W.D. Scharfe, W. Rath, Lasers for industrial applications in material processing, Materials Science Forum 301 (1999) 253–286.

[7] S.H. Kim, I.B. Sohn, S. Jeong, Ablation characteristics of aluminum oxide and nitride ceramics during femtosecond laser micromachining, Applied Surface Science 255 (2009) 9717–9720.